Comparative ability of EDTA, GLDA, and MGDA to desorb Pb from contaminated montmorillonite: Aging effects

Mehran Shirvani (shirvani@iut.ac.ir)
Isfahan University of Technology https://orcid.org/0000-0003-0297-053X
Farzad Parsadoust
Isfahan University of Technology
Hossein Shariatmadari
Isfahan University of Technology
Mohammad Dinari
Isfahan University of Technology

Research Article

Keywords: Chelating agents, Pb complexation, Pb desorption, Residence time

Posted Date: March 1st, 2022

DOI: https://doi.org/10.21203/rs.3.rs-1380841/v1

Comparative ability of EDTA, GLDA, and MGDA to desorb Pb from contaminated montmorillonite: Aging effects

Farzad Parsadoust[1], Mehran Shirvani[1*], Hossein Shariatmadari[1], Mohammad Dinari[2]

[1]Department of Soil Science, College of Agriculture, Isfahan University of Technology, Isfahan 84156-83111, Iran

[1]Department of Chemistry, Isfahan University of Technology, Isfahan 84156-83111, Iran.

*Corresponding author,

Tel: +98 3133913480

Email: shirvani@cc.iut.ac.ir

ORCID: 0000-0003-0297-053X

Abstract

Study of Pb desorption processes from clay minerals by chelating ligands is crucial to better understand the fate and transport of Pb in soil and sediment environments. In this study, Pb desorption from a Pb-loaded montmorillonite (MMT) was studied as affected by ethylenediaminetetraacetic acid (EDTA) and its two alternative eco-friendly chelating agents, i.e., methylglycine diacetic acid (MGDA) and glutamic-*N*,*N*-diacetic acid (GLDA) at two concentrations of 0.25 and 1.0 mM. The impacts of a 30-day residence time on the rate and quantity of Pb desorption were also evaluated. The result showed that Pb desorption kinetics was biphasic with an initial rapid phase, lasting for about 3 h, followed by a slow phase, lasting to 12 h. The degree of Pb desorption from Ca-MMT was proven to be governed by the nature and concentration of the chelating ligands presented in the systems. The capacity of the ligands to desorb Pb from Ca-MMT was in the order EDTA >> MGDA > GLDA, according to the decreasing order in the stability constants of their complexes with Pb ions. The aging of the MMT systems caused a significant reduction in both Pb desorption quantity and rate parameters. The results suggest that EDTA would have a more serious Pb-mobilizing impact than GLDA and MGDA in contaminated soil and sediments which contain Ca-MMT as a major clay constituent.

Keywords: Chelating agents; Pb complexation, Pb desorption; Residence time.

1. Introduction

Lead (Pb) is among the most toxic heavy metals released into the environment, mostly from anthropogenic activities, such as vehicular traffic, mining, smelting, heating, and improper waste recycling and disposal (Natasha et al. 2020). Lead ions entering the soil can be absorbed by plants or leached into the surface and ground waters and eventually accumulate in the human body through the food chain and water intake, causing various toxic effects on nervous, renal, digestive, and reproductive organs (Meena et al. 2020).

In soil and sediment systems, Pb ions are predominantly adsorbed by clay particles (Carocci et al. 2016). Therefore, Pb bioavailability, mobility, and toxicity in soils and sediments depend on the desorption quantity and rate of the pre-adsorbed Pb on the clay minerals (Strawn &Sparks 1999). Montmorillonite (MMT) is a typical mineral found in many soils and sediments, controlling the mobility and bioavailability of metals through adsorption-desorption reactions (Murray, 2006). There are some reports on the adsorption of Pb by MMT, in which chemical binding of Pb ions on surface hydroxyl groups and electrostatic attraction of Pb cations on the permanent negatively charged sites have been proposed as the main mechanisms for Pb adsorption on MMT surfaces. (Li et al. 2012, Parsadoust et al. 2020, Zhang &Hou 2008a, Zhu et al. 2011). However, desorption processes of Pb from MMT, which is important in predicting the fate and transport of Pb in soil and subsurface systems, and the factors controlling the desorption processes, have not been studied adequately.

Residence time of metal ions in soil and sediment systems is one of the most important factors which determine the adsorption reversibility of metals. Desorption of metal ions from the minerals usually decreases with increasing the contact time between the ions and the minerals (Garman et al. 2007, Srivastava et al. 2007). Slow diffusion and trapping of the metal ions into the

mineral lattice and internal spaces, movement of the ions to sites with higher binding energies, and surface precipitation are the suggested processes responsible for the reduction of metal desorption with time (Barrow et al. 2012). However, studies that describe the influence of aging on Pb desorption behavior from MMT are scarce.

Organic ligands, especially the chelating ligands, can also affect Pb desorption processes from minerals (Đolić et al. 2015). Various natural and synthetic organic ligands enter the soil and water bodies and significantly enhance desorption of Pb from the mineral surfaces with a potential risk for metal contamination of groundwater or uptake by plants (Shahid et al. 2012). The chelating ligands form stable complexes with both aqueous and surface-bound metal cations, making them more mobile and available for plant uptake. Ethylenediaminetetraacetic acid (EDTA) and its biodegradable alternatives such as glutamic-*N*,*N*-diacetic acid (GLDA) and methylglycinediacetic acid (MGDA) are the chelating ligands widely used in various applications, including water softening, textile manufacturing, cosmetic formulations, food processing, polymer production, metal plating, gas sweetening, and pulp and paper manufacturing (Hart 2000, Raynie 2020). As a result, these ligands are discharged into the environment with the sewage water of industrial and domestic origin (European Chemical Bureau 2004). Moreover, these ligands are applied for soil washing and chelant-assisted phytoremediation practices to mobilize metals in contaminated soils (Guo et al. 2018, Qiao et al. 2017). The enhancing role of EDTA in desorbing Pb from MMT has been revealed in some studies (Saha et al. 2003, Shahid et al. 2014, Zhang &Hou 2008b) however, our knowledge regarding the role of GLDA and MGDA in Pb desorption from MMT is limited.

Characterization of Pb desorption processes from clay minerals, particularly in aged systems, is of interest because this information is necessary to better understand the fate, transport, and ecological risk of the metals in soil and sediment environments. Therefore, this study was

performed to compare the impacts of EDTA and its eco-friendly alternatives, i.e., GLDA and MGDA, on Pb desorption from aged and non-aged Pb-contaminated MMT clay.

2. Materials and methods

2.1. Materials

Montmorillonite STx-1b (Gonzales County, Texas, USA) was purchased from Source Clay Repository of Clay Minerals Society (Purdue University, USA) and applied in this study.

N, N-bis(carboxylatomethyl)-L-glutamate tetrasodium (Na_4GLDA, CAS Number: 51981-21-6) and methyl-glycine diacetate trisodium (Na_3MGDA, CAS Number: 164462-16-2) were both from TCI Chemical Co. (Tokyo, Japan), ethylenediaminetetraacetate disodium dihydrate ($Na_2EDTA.2H_2O$, CAS Number: 6381-92-6) from the Samchun Chemical Co. Inc. (Gyeonggi-do, Korea). Lead nitrate ($Pb(NO_3)_2$) was purchased from Merck (Darmstadt, Germany).

2.2. Lead adsorption

To obtain Pb adsorption isotherms, 0.2 g MMT samples were added to centrifuge tubes with 20 mL of 0.005 *M* $CaCl_2$ solution containing 0, 0.1, 0.2, 0.3, 0.4, 0.7, 1.0, 1.5, 2 and 2.5 mmol Pb L^{-1} in triplicate. For each Pb concentration a control was also run without MMT addition. Subsequently, the samples were shaken at 25 °C in orbital incubator-shaker set at 180 rpm. After 24 h of shaking, the suspensions were centrifuged at 2500 rpm for 10 min and the separated supernatants were tested for their pH values and analyzed for Pb concentrations using a Perkin Elmer 3030 atomic absorption spectrometer (AAS) with a detection limit of 0.005 mg L^{-1}. The Pb adsorbed on each clay sample was estimated from the difference between the initial and equilibrium Pb concentrations using a mass balance calculation as follows:

$$q = (C_0 - C_e)\frac{V}{M} \quad (1)$$

where, q is the quantity of Pb adsorbed (mmol kg^{-1}); C_0 and C_e are the initial and final Pb concentrations (mmol L^{-1}), respectively, V represents the experimental solution volume (L), and M is the clay mass (kg).

The adsorption data were subsequently fitted by the Langmuir model shown as follows:

$$q_e = \frac{K_L q_m C_e}{1 + K_L C_e} \quad (2)$$

where, q_e (mmol kg^{-1}) is the amount of Pb adsorbed on the MMT at equilibrium, C_e (mmol L^{-1}) is the Pb concentration at equilibrium, q_m (mmol kg^{-1}) is adsorption capacity of the clay, and K_L (L $mmol^{-1}$) is a constant related to the adsorption affinity.

The PHREEQC geochemical model (version 2.18.00) was applied to estimate the dominant Pb species in equilibrium solutions. The saturation index (SI) was also calculated according to Eq. 3, to determine if the solutions were supersaturated with respect to the Pb minerals.

$$SI = \log(\frac{IAP}{K_{sp}}) \quad (3)$$

where, IAP is the ion activity product and K_{sp} is the solubility product constant of the mineral. A negative SI value indicates under-saturation, while a positive SI value represents super-saturation, with respect to a given mineral.

2.3. Preparation of Pb-loaded MMT samples

A series of Pb-loaded MMT samples were prepared using the batch method. Montmorillonite (0.2 g) samples were placed into 50 mL polypropylene centrifuge tubes and treated with 20 mL of 0.005 *M* $CaCl_2$ background solutions containing 2.5 mmol L^{-1} of Pb. The samples were shaken for 24 h in an orbital incubator-shaker set at 25 °C and 180 rpm.

Subsequently, the solutions were separated from the Pb-loaded MMT samples using centrifugation at 2500 rpm for 10 min, and collected in 25 mL vials. The clay residues remaining in the centrifuge tubes were carefully washed with deionized water to remove the entrained Pb ions from the clay samples, and the rinsates were combined with the previously-collected supernatants to make up a final volume of 25 mL. The Pb concentrations in the supernatants were determined using the AAS. Finally, the Pb adsorbed on each clay sample was estimated from the difference between the initial and final Pb concentrations using a mass balance calculation from Eq. 1.

2.4. Effects of chelating ligands on Pb desorption

The impacts of GLDA, MGDA, and EDTA chelating agents on Pb desorption kinetics from MMT were studied in triplicates. The Pb-loaded mineral samples were extracted with 20 mL of 0.005 M $CaCl_2$ solutions containing 0, 0.25, and 1 mM GLDA, MGDA, and EDTA ligands. The samples were shaken at 180 rpm and 25 °C in the incubator-shaker for selected periods of 0.25, 0.5, 1, 1.5, 3, 6, 12, and 24 h before being centrifuged. At the end of each shaking time, Pb concentration in the supernatants was determined using the AAS. Finally, the amounts of Pb desorbed from the clay samples were calculated and plotted versus time for each system.

2.5. Effect of aging on Pb desorption

To determine the aging effect on Pb desorption, a set of Pb-loaded minerals was incubated for 30 days at 25 °C and 60% water holding capacity. The aged samples were then treated with 20 mL of 0.005 M $CaCl_2$ solution containing 0, 0.25, and 1 mM of GLDA, MGDA, and EDTA ligands for different periods, as described above for nonaged samples. At the end of each shaking time, Pb

concentration in the supernatants was determined using the AAS. Finally, the amounts of Pb desorbed from the clay samples were calculated and plotted versus time for each system.

The pseudo-first-order, pseudo-second-order, Elovich, parabolic diffusion and power function models were examined to describe the kinetic data, among which the pseudo-second-order was found to be the best fitted model and hence was applied in this study. The pseudo-second-order model was introduced by Eq. (2) below (Ho &McKay 1999):

$$q_t = \frac{k_2 q_e^2 t}{1 + k_2 q_e t} \tag{4}$$

where, q_t and q_e represent the Pb desorbed (mmol kg^{-1}) at time t (h) and equilibrium, respectively, and k_2 (kg $mmol^{-1}$ h^{-1}) is the pseudo-second-order rate constant. The *"initial desorption rate"* (h) (mmol kg^{-1} h^{-1}) was also obtained using the Eq. 3, derived from the pseudo-second-order model:

$$h = k_2 q_e^2 \tag{5}$$

The instantaneous Pb desorption rate at unit time (DR_1) was also calculated for each system from the slope of the fitted pseudo-second-order model determined using the first derivative of the curve (Eq. 4) at t=1 h:

$$\frac{dq_t}{dt} = \frac{k_2 q_e^2}{(1 + k_2 q_e t)^2} \tag{6}$$

2.6. Statistical analysis and curve fitting methods

The Curve fitting and graph preparations were carried out using the Graph Pad Prism (version 5.04, San Diego, California, USA). Adequacy of the kinetic models describing the time-dependent Pb desorption data was evaluated by two goodness-of-fit criteria, namely the determination coefficient (R^2) and absolute sum of squares (ASS).

One-way ANOVA with repeated measures followed by the Tukey's multiple comparison analysis in Graph Pad Prism statistical package were used to examine if the quantity of Pb desorbed from the MMT in nonaged and 30-day-aged samples in the presence of GLDA, MGDA, and EDTA ligands were significantly different from each other.

3. Results and Discussions

3.1. Lead adsorption on MMT

Lead adsorption isotherm data were significantly (R^2=0.98, P<0.01) fitted by the Langmuir model (Fig. 1). The maximum Pb adsorption capacity of MMT, estimated from the Langmuir q_m parameter, was 143.3 mmol kg^{-1} and the Langmuir affinity constant (K_L) was 7.93 L kg^{-1}. Speciation calculations showed that the SI values for all systems were negative (Table 1), confirming that the equilibrium solutions were all under-saturated with respect to the Pb-bearing minerals. This finding might be because of the high adsorption capacity of MMT which reduces the Pb concentrations in solutions to low levels enough to restrict the formation of any precipitate. The free Pb^{2+} ion was the major species (82%) and $PbCl^+$ was the second most predominant (17%) Pb species in the equilibrium solutions (Table 1).

The equilibrium pH value of the MMT suspensions decreased with increasing Pb adsorption (Fig. 1), suggesting the replacement of protons of the -OH functional groups on the mineral edge surfaces by the Pb ions through inner-sphere complexation and subsequent release of H^+. In addition, hydrolysis of Pb^{2+} during adsorption can be an important source of H^+ released as described by the following surface complexation reaction (Bargar et al. 1997):

$$\equiv S\text{-}OH + Pb^{2+}_{(aq)} + H_2O \leftrightarrow \equiv S\text{-}O\text{-}Pb(OH)^+ + 2H^+$$

where, S represents the MMT's constituent cations (i.e., Al^{3+}, Si^{4+}, Mg^{2+}, and Fe^{3+}) and S-OH is a surface functional group.

3.2. Lead desorption pattern

The Pb desorption data from MMT is shown in Fig. 2. As can be seen, the Pb desorption was biphasic, with a fast initial phase that lasted for about 3 hours, followed by a much slower phase that spanned the rest of the experimental period. The kinetic behavior observed was similar to our previous kinetic study on Cd desorption from palygorskite and sepiolite clay minerals (Shirvani et al. 2007). The Pb desorbed during the initial 3-hour period was at least 68% of the total Pb desorbed from MMT. The initial faster Pb desorption phase most likely indicated the desorption of exchangeable Pb ions from the adsorption sites of lower bonding energy on MMT's surfaces (Kandpal et al. 2005). The high abundance of weakly-adsorbed Pb ions at the initial phase generates a greater driving force of the concentration gradient at the mineral−liquid interface, leading to an enhanced Pb desorption rate (Li et al. 2012). The slower desorption phase may be attributed to Pb release from specific surface sites with higher desorption activation energy as well as various diffusion-limited desorption reactions (Sparks 2018).

The total quantity of Pb desorbed after 24 h from the MMT sample was 13.0 mmol kg^{-1} representing about 10% of the total Pb (131.7 mmol kg^{-1}) loaded on the MMT (Fig. 2). This finding indicates that some reactions involved in the Pb sorption processes may be irreversible or very slowly-reversible, which can be attributed to the strong Pb binding to the high-affinity sites on the clay surfaces or diffusion into the clay interlayer spaces (Strawn &Sparks 1999). Similarly, Undabeytia et al. (2002) contributed the high irreversibility of Cu adsorption on montmorillonite to the large affinity of the metal ions for edge site positions. Tang et al. (2009) and Wang et al.

(2011) also showed that Pb sorption on kaolin was almost irreversible, with only less than 5% of the adsorbed Pb being able to be desorbed.

The time-dependent Pb desorption data were successfully described by the pseudo-second-order model, according to the significant R^2 values presented in Tables 2 and 3. This finding suggests that surface desorption rather than bulk diffusion may be the rate-limiting step in the Pb release process (Avila et al. 2010).

3.3. Ligand effects on Pb desorption

The presence of GLDA, MGDA, and EDTA significantly (P<0.05) increased the quantity of Pb desorbed from MMT into the solution. However, EDTA had a significantly higher ability to remove Pb from the MMT compared with GLDA and MGDA. For instance, the total quantity of Pb desorbed (DQ_t) from MMT was 13.04 mmol kg^{-1} in the ligand-free system, which significantly (P<0.05) increased to 17.16, 27.59, and 33.72 mmol kg^{-1} with 0.25 mM of GLDA, MGDA, and EDTA, respectively (Fig. 3). These values reveal that only 9.1%, 12.0%, 19.3%, and 23.5% of the sorbed Pb were desorbed in the absence and presence of 0.25 mM of GLDA, MGDA, and EDTA, respectively, within the 24-h period.

In the presence of 1.00 mM of the ligands, the highest Pb desorption percentage was induced by EDTA (92.9%), followed by MGDA (58.9%), and then GLDA (46.6%), which were significantly (P<0.05) different from each other (Fig. 3). The noticeably greater effectiveness of EDTA compared with GLDA and MGDA in Pb desorption was presumably related to the ability of EDTA to form remarkably more stable chelates with Pb ions. Ligands EDTA, MGDA, and GLDA have a 1:1 stability constant with Pb of 10^{18}, $10^{12.1}$, and $10^{10.5}$, respectively (Kołodyńska 2011). The formation of stable non-adsorbing chelates in the solution

lowers the free metal ion activity, leading to metal ion desorption from the solid surfaces (Violante 2013). Moghal et al. (2019) also reported that the desorption efficiency of Pb by EDTA from soils was in the range of 69–93%.

The maximum Pb desorption quantity at equilibrium (q_e) determined by the fitted pseudo-second-order model was 12.93 mmol kg^{-1} in control (ligand-free) system, which increased to 15.46, 25.50, and 34.19 mmol kg^{-1} in the presence of 0.25 mM of GLDA, MGDA, and EDTA, respectively (Table 2). The corresponding q_e values in the presence of 1.00 mM of the ligands were 66.17, 82.69, and 128.5 mmol kg^{-1}, respectively (Table 3). Hence, the Pb desorption potential of the ligands from MMT followed the order EDTA >>MGDA >GLDA. These findings may implicate a much higher Pb mobilizing effect of EDTA compared to those of GLDA and MGDA in contaminated soils and sediments containing high amounts of MMT.

The Pb desorption rate from MMT was also affected by the chelating ligands. The initial Pb desorption rate (h) estimated from the pseudo-second-order model in the presence of 0.25 mM GLDA, MGDA, and EDTA was 33.46, 69.67, and 78.32 mmol kg^{-1} h^{-1}, respectively, which was higher than that obtained in the ligand-free system as 31.76 mmol kg^{-1} h^{-1} (Table 2). The corresponding "h" values at the ligand concentrations of 1.00 mM were 83.19, 205.1, and 660.5 mmol kg^{-1} h^{-1}, respectively (Table 3), indicating the extremely high Pb desorption rate induced by EDTA. The Pb desorption rate at t=1 h (DR_1) was also the highest in the systems affected by EDTA, followed in decreasing order by the systems containing MGDA, GLDA, and no ligand, respectively (Tables 2 and 3). In general. the enhancing effect of the ligands on Pb desorption rate was in the order of EDTA >> MGDA> GLDA, which is in accordance with the order of the complexation capacity of the ligands. The higher Pb desorption rate from MMT in the presence of EDTA could indicate a higher potential of Pb pollution hazard in MMT-rich metal polluted soils.

From a phytoextraction point of view, however, the greater values of Pb desorption rate constants obtained in the systems receiving ligands suggest more rapid resupply of Pb from soil minerals following local depletion through plant uptake during ligand-assisted phytoextraction practices.

3.4. Aging effects on Pb desorption

Incubating the Pb-loaded MMT samples for 30 days caused a decrease not only in the proportions of Pb desorbed but also in Pb desorption rates. The effect of aging on the Pb desorption kinetics from MMT in the presence of GLDA, MGDA, and EDTA ligands is shown in Fig. 2. Similar to the case of nonaged systems, the kinetic patterns of Pb desorption from the aged samples showed an initial rapid desorption phase lasting for about 3 h, which may be referred to as the Pb ions retained by the low-energy surface sites (Strawn &Sparks 1999), followed by a slower phase over the remaining 24 h. Indeed, extending the release time from 3 h to 24 h only slightly increased the amounts of Pb desorbed from MMT.

The DQ_t values obtained for the systems with and without the aging process (Fig. 3) showed statistically significant (P<0.05) differences, indicating that the maximum amount of Pb desorbed remarkably declined after aging. For example, the DQ_t value in the ligand-free system decreased from 13.04 mmol kg^{-1} in the nonaged sample to 2.75 mmol kg^{-1} in the aged sample, indicating 3.7 times lower Pb desorption after aging. The aging treatment also caused the DQ_t value to be significantly (P<0.05) decreased by 5.2, 4.8, and 5.6 times in the presence of 0.25 mM of GLDA, MGDA, and EDTA, respectively (Fig. 3). The DQ_t values in the systems containing 1.00 mM of the chelating ligands also showed a decreasing trend with aging (Fig. 3). This finding can be attributed to the transfer of Pb ions from low-energy sites to high-energy sites and the movement of Pb ions to the less accessible sites for ligands during the 30 days of incubation (Sparks 2018).

The aging process also affected the quantity of Pb desorbed at equilibrium (q_e). The q_e value estimated from the pseudo-second-order model was 15.46, 25.50, 34.19 mmol kg^{-1} at 0.25 mM of GLDA, MGDA, and EDTA ligands, respectively, which reduced to 3.08, 3.69, 9.75 mmol kg^{-1}, respectively, after the aging process (Table 2). At the concentration of 1.00 mM of the ligands, the q_e value decreased from 66.17, 82.69, and 128.5 mmol kg^{-1} to 13.67, 25.08, and 69.74 mmol kg^{-1}, respectively, after 30 days of incubation (Table 3), indicative of the increasing Pb retention irreversibility with time.

The rate of Pb desorbed from the MMT was significantly decreased due to the sample aging (Tables 2 and 3). For example, in the ligand-free systems, aging caused decreases of h value from 30.42 to 5.66 mmol kg^{-1} h^{-1} and DR_1 value from 9.22 to 1.82 mmol kg^{-1} h^{-1}, suggestive of a significantly higher irreversible or slowly-reversible fraction of the sorbed Pb in the aged systems compared to the nonaged ones.

Aging also reduced the rate parameters in the presence of the chelating ligands at both concentrations of 0.25 and 1.00 mM. The enhancing effect of the ligands on Pb desorption in the aged systems was quite similar to that observed in the nonaged systems followed the order: EDTA> MGDA> GLDA, obeying the order of their formation constants of the complexes formed with Pb ions. For example, at a concentration of 0.25 mM of the GLDA, MGDA, and EDTA ligands, the initial rate (h) value decreased from 33.46, 69.67, and 78.32 mmol kg^{-1} h^{-1} to 9.96, 12.52, and 30.42 mmol kg^{-1} h^{-1}, respectively, after aging (Table 2). The same decreasing effects of aging on the Pb desorption rate were also observed in the systems containing 1.00 mM of the chelating ligands (Table 3). Hence, Pb is more slowly desorbed from MMT into the solution phase after aging.

4. Conclusion

This study explored the impacts of EDTA, MGDA, and GLDA ligands on Pb desorption from the aged and nonaged MMT. The results showed biphasic kinetics in Pb desorption processes and substantial irreversibility in Pb retention by MMT. The results also reveal that aging significantly reduced both the quantity and rate of Pb desorption from MMT. Although GLDA and MGDA ligands enhanced the Pb desorption, they have a rather smaller ability compared to EDTA to desorb Pb from MMT. Hence, it is expected that these eco-friendly ligands will have a considerably lower potential than EDTA to mobilize toxic Pb ions from soils and sediments containing MMT as a major component.

Statements and Declarations

Availability of data and materials (data transparency)

The datasets generated during and/or analysed during the current study are available from the corresponding author on reasonable request.

Funding

This research was funded by Isfahan University of Technology.

Competing Interests

The authors declare that they have no known competing financial interests or personal relationships that could have appeared to influence the work reported in this paper.

CRediT

Farzad Parsadoust: Investigation, Writing- Original draft; Mehran Shirvani: Supervision, Validation, Writing- Reviewing and Editing; Hossein Shariatmadari: Review & Editing; Mohammad Dinari: Formal analysis, Reviewing and Editing.

Authors' Contributions

All authors contributed to the study conception and design. Material preparation, data collection and analysis were performed by Farzad Parsadoust and Mohammad Dinari. The first draft of the manuscript was written by Farzad Parsadoust and all authors commented on previous versions of the manuscript. All authors read and approved the final manuscript.

Code availability

No any special code was applied in the study.

Ethics approval

No animals or human participants, their data or biological materials were included in the study.

Consent to participate

This research did not involve human participants, identifiable human data or human tissue.

Consent for publication

This research did not involve human participants, identifiable human data or human tissue.

References

Avila RE, Peña LA, Jiménez JC (2010) Surface desorption and bulk diffusion models of tritium release from Li2TiO3 and Li2ZrO3 pebbles. J Nucl Mater 405, 244-251

Bargar JR, Brown GE, Parks GA (1997) Surface complexation of Pb(II) at oxide-water interfaces: I. XAFS and bond-valence determination of mononuclear and polynuclear Pb(II) sorption products on aluminum oxides. Geochim Cosmochim Acta 61, 2617-2637

Barrow NJ, Brümmer GW, Fischer L (2012) Rate of desorption of eight heavy metals from goethite and its implications for understanding the pathways for penetration. Eur J Soil Sci 63, 389-398

Carocci A, Catalano A, Lauria G, Sinicropi MS, Genchi G (2016) Lead Toxicity, Antioxidant Defense and Environment. In: de Voogt P (Editor), Reviews of Environmental Contamination and Toxicology Volume 238. Springer International Publishing, Cham, pp. 45-67

Đolić MB, Rajaković-Ognjanović VN, Marković JP, Janković-Mandić LJ, Mitrić MN, Onjia AE, Rajaković LV (2015) The effect of different extractants on lead desorption from a natural mineral. Appl Surf Sci 324, 221-231

European Chemical Bureau (2004) European Union Risk Assessment Report, edetic acid (EDTA). European Chemicals Bureau, Dortmund, Germany

Garman SM, Eick MJ, Beck M (2007) Desorption kinetics of lead from goethite: Effect of residence time and mixing. Soil Sci 172, 177-188

Guo X, Zhang G, Wei Z, Zhang L, He Q, Wu Q, Qian T (2018) Mixed chelators of EDTA, GLDA, and citric acid as washing agent effectively remove Cd, Zn, Pb, and Cu from soils. J Soils Sediments 18, 835-844

Hart JR (2000) Ethylenediaminetetraacetic acid and related chelating agents. In: Ley C (Editor), Ullmann's Encyclopedia of Industrial Chemistry. Wiley-VCH Verlag GmbH & Co. KGaA, Weinheim, Germany

Ho YS, McKay G (1999) Pseudo-second order model for sorption processes. Process Biochemistry 34, 451-465

Kandpal G, Srivastava PC, Ram B (2005) Kinetics of desorption of heavy metals from polluted soils: influence of soil type and metal source. Water Air Soil Pollut 161, 353-363

Kołodyńska D (2011) Chelating agents of a new generation as an alternative to conventional chelators for heavy metal ions removal from different waste waters. In: Ning R (Editor), Expanding issues in desalination. Intech, Rijeka, Croatia, pp. 339-371

Li Y, Wang J-d, Wang X-j, Wang J-f (2012) Adsorption–desorption of Cd(II) and Pb(II) on Ca-montmorillonite. Ind Eng Chem Res 51, 6520-6528

Meena V, Dotaniya ML, Saha JK, Das H, Patra AK (2020) Impact of Lead Contamination on Agroecosystem and Human Health. In: Gupta DK, Chatterjee S , Walther C (Editors), Lead in Plants and the Environment. Springer International Publishing, Cham, pp. 67-82

Moghal AAB, Mohammed SAS, Almajed A, Al-Shamrani MA (2019) Desorption of Heavy Metals from Lime-Stabilized Arid-Soils using Different Extractants. Int J Civ Eng

Natasha, Dumat C, Shahid M, Khalid S, Murtaza B (2020) Lead Pollution and Human Exposure: Forewarned is Forearmed, and the Question Now Becomes How to Respond to the Threat! In: Gupta DK, Chatterjee S , Walther C (Editors), Lead in Plants and the Environment. Springer International Publishing, Cham, pp. 33-65

Parsadoust F, Shirvani M, Shariatmadari H, Dinari M (2020) Effects of GLDA, MGDA, and EDTA chelating ligands on Pb sorption by montmorillonite. Geoderma 366, 114229

Qiao J, Sun H, Luo X, Zhang W, Mathews S, Yin X (2017) EDTA-assisted leaching of Pb and Cd from contaminated soil. Chemosphere 167, 422-428

Raynie DE (2020) Innocuous and Less Hazardous Reagents. In: de la Guardia M , Salvador G (Editors), Challenges in Green Analytical Chemistry. Royal Society of Chemistry, Croydon, UK, pp. 92

Saha UK, Iwasaki K, Sakurai K (2003) Desorption behavior of Cd, Zn and Pb sorbed on hydroxy aluminum and hydroxy aluminosilicate-montmorillonite complexes. Clays Clay Miner 51, 481-492

Shahid M, Pinelli E, Dumat C (2012) Review of Pb availability and toxicity to plants in relation with metal speciation; role of synthetic and natural organic ligands. J Hazard Mater 219-220, 1-12

Shahid M, Austruy A, Echevarria G, Arshad M, Sanaullah M, Aslam M, Nadeem M, Nasim W, Dumat C (2014) EDTA-Enhanced Phytoremediation of Heavy Metals: A Review. Soil Sediment Contam 23, 389-416

Shirvani M, Shariatmadari H, Kalbasi M (2007) Kinetics of cadmium desorption from fibrous silicate clay minerals: Influence of organic ligands and aging. Appl Clay Sci 37, 175-184

Sparks DL (2018) Kinetics and mechanisms of chemical reactions at the soil mineral water interface. In: Sparks DL (Editor), Soil Physical Chemistry. CRC Press, Boca Raton, FL, pp. 147-204

Srivastava P, Gräfe M, Singh B, Balasubramanian M (2007) Cadmium and Lead Desorption from Kaolinite. In: Barnett MO , Kent DB (Editors), Developments in Earth and Environmental Sciences. Elsevier, pp. 205-233

Strawn D, Sparks D (1999) Sorption Kinetics of Trace Elements in Soils and Soil Materials. In: Selim H , Iskandar K (Editors), Fate and Transport of Heavy Metals in the Vadose Zone. Lewis Publishers, Boca Raton, FL, pp. 1–28

Undabeytia T, Nir S, Rytwo G, Serban C, Morillo E, Maqueda C (2002) Modeling adsorption−desorption processes of Cu on edge and planar sites of montmorillonite. Environ Sci Technol 36, 2677-2683

Violante A (2013) Elucidating mechanisms of competitive sorption at the mineral/water interface. In: Sparks DL (Editor), Advances in agronomy. Academic Press, pp. 111-176

Zhang SQ, Hou WG (2008a) Adsorption behavior of Pb(II) on montmorillonite. Colloids Surf A 320, 92-97

Zhang SQ, Hou WG (2008b) Adsorption behavior of Pb (II) on montmorillonite. Colloids Surf A Physicochem Eng 320, 92-97

Zhu J, Cozzolino V, Pigna M, Huang Q, Caporale AG, Violante A (2011) Sorption of Cu, Pb and Cr on Na-montmorillonite: Competition and effect of major elements. Chemosphere 84, 484-489

Figure captions

Figure 1. Experimental Pb adsorption isotherm data (fitted by the Langmuir equation, q_m=143.3 mmol kg^{-1}, K_L=7.93 L kg^{-1}, R^2=0.98, P<0.01) and changes of pH value as a function of equilibrium Pb concentration in montmorillonite suspensions. (adsorbent dose, 10 g L^{-1}; temperature, 25 °C). Error bars are too small to be visible.

Figure 2. Effects of GLDA, MGDA, and EDTA at two concentrations of 0.25 mM (A and B) and 1.00 mM (C and D) on time-dependent Pb desorption from nonaged (A and C) and aged (B and D) Pb-loaded montmorillonite. Symbols represent experimental data and lines represent fitted pseudo-second-order kinetic model. Error bars are too small to be visible.

Figure 3. The total quantity of Pb desorbed (DQ_t) from the non-aged and aged Pb-loaded montmorillonite in the presence of GLDA, MGDA, and EDTA ligands at two concentrations of 0.25 mM (A) and 1.00 mM (B). Each bar is the mean ± SD of the results from three replications. Different lower-case letters in each diagram indicate significant differences at $p \leq 0.05$ (Tukey test) in DQ_t

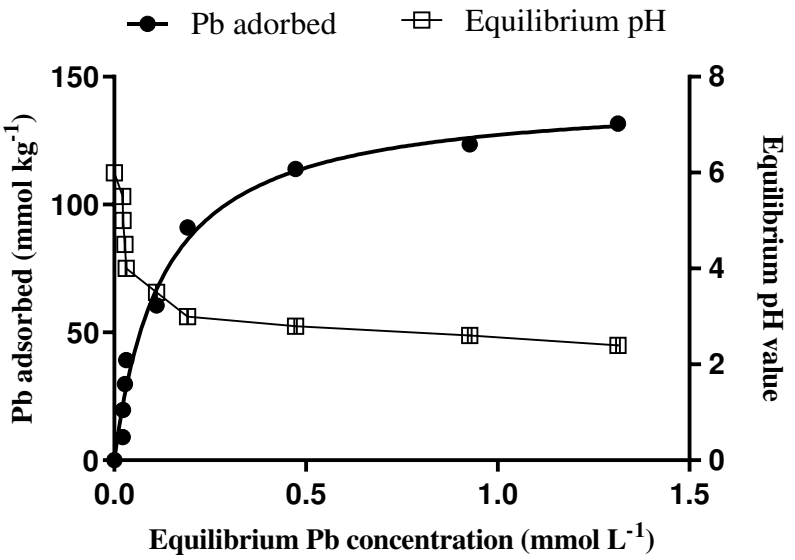
Pb adorbed
Equilibrium pH
Pb adsorbed (mmol kg-1)
Equilibrium pH value
Equilibrium Pb concentration (mmol L-1)
150
100
50
0
8
6
4
2
0
0.0
0.5
1.0
1.5

Figure 1

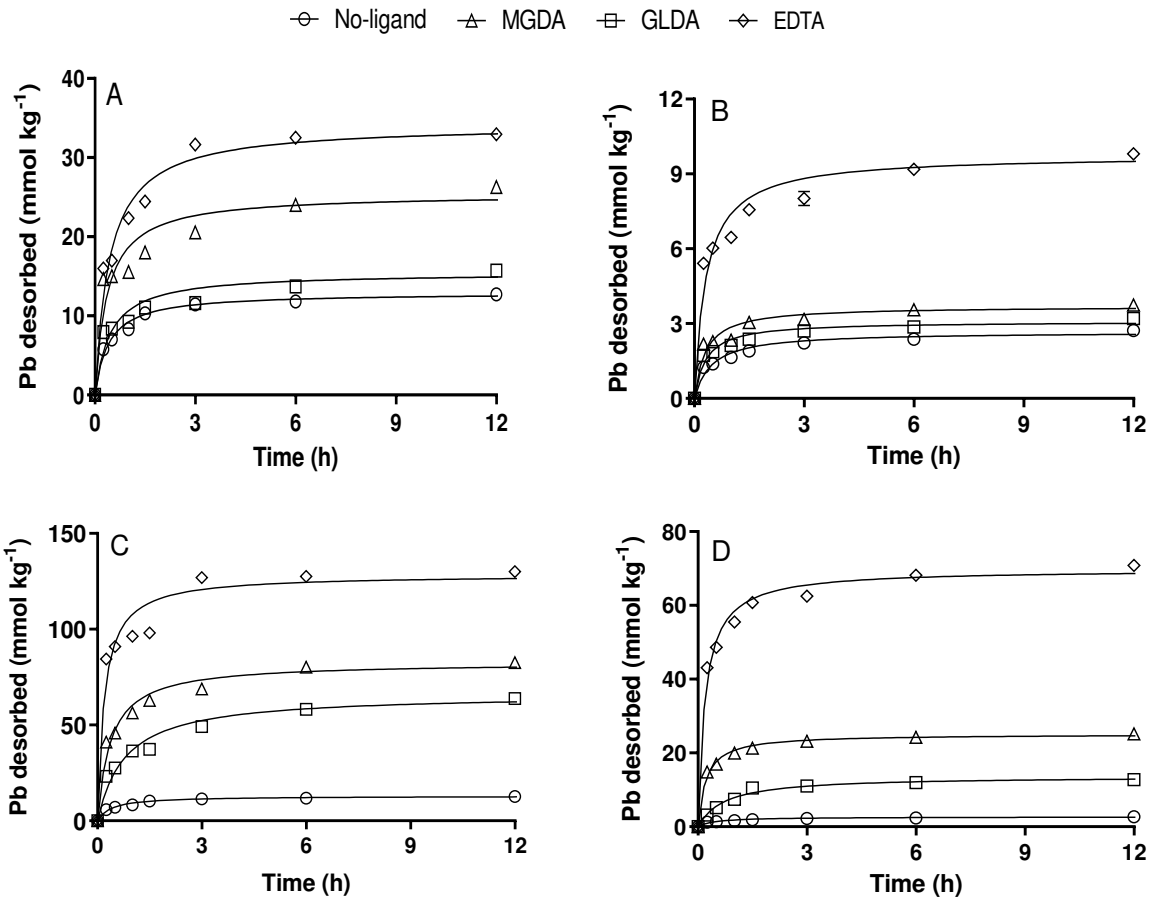
No-ligand
MGDA
GLDA
EDTA
A
B
C
D
Pb desorbed (mmol kg-1)
Time (h)
0
3
6
9
12
10
20
30
40
50
100
150
60
80

Figure 2

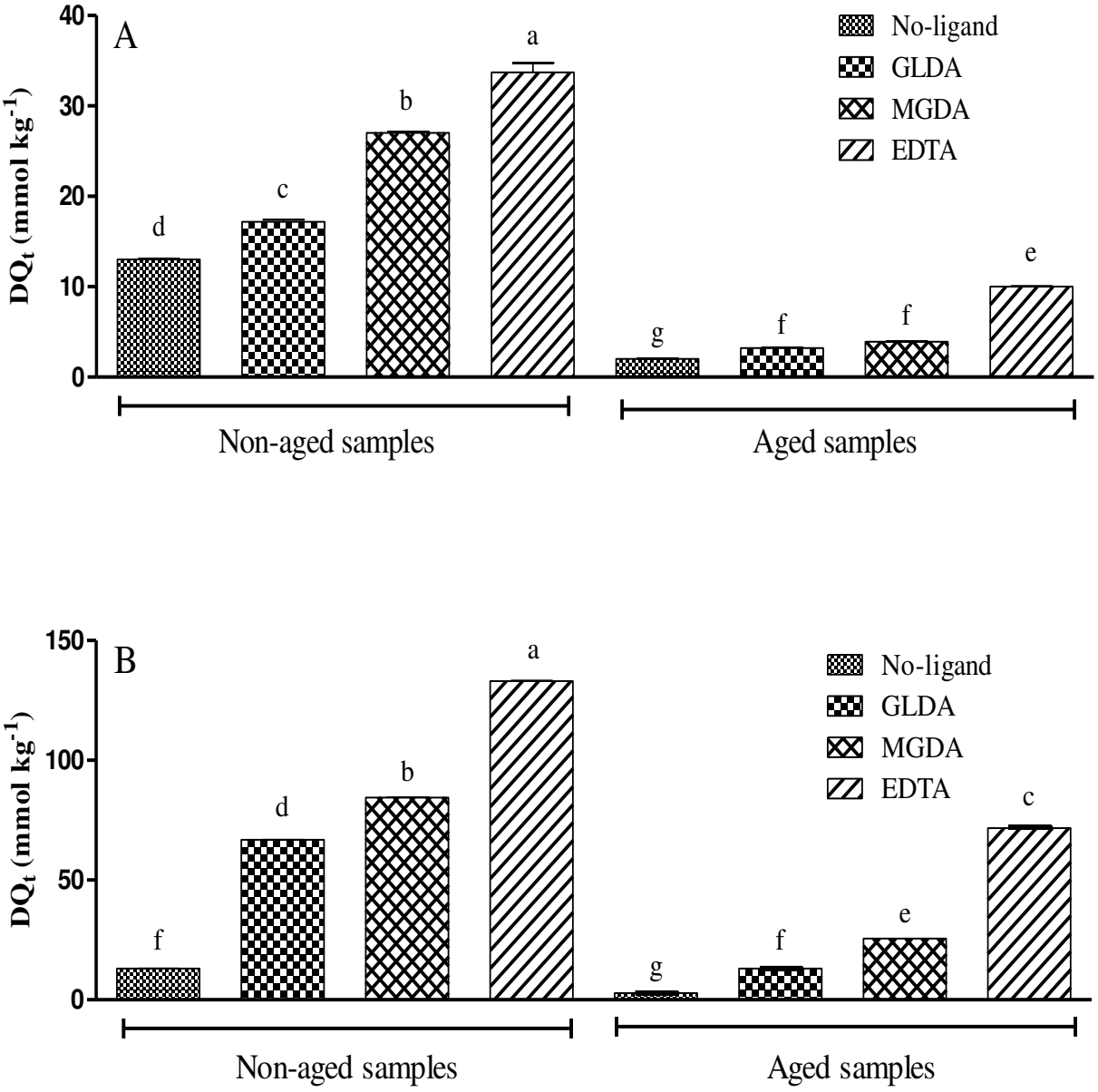
A
B
No-ligand
GLDA
MGDA
EDTA
DQt (mmol kg-1)
Non-aged samples
Aged samples
a
b
c
d
e
f
g

Figure 3

Table 1. Dominant soluble Pb species in equilibrium solutions and saturation indices estimated by PHREEQC speciation program. Values in parenthesis represent percentage of total soluble Pb.

	Pb concentration (mM)								
	0.022	0.023	0.028	0.031	0.11	0.19	0.47	0.93	1.31
Dominant soluble species	Pb^{2+} (81.7%)	Pb^{2+} (82.0%)	Pb^{2+} (82.1%)	Pb^{2+} (82.2%)	Pb^{2+} (82.1%)	Pb^{2+} (82.1%)	Pb^{2+} (82.0%)	Pb^{2+} (82.0%)	Pb^{2+} (82.0%)
	$PbCl^{+}$ (17.6%)	$PbCl^{+}$ (17.6%)	$PbCl^{+}$ (17.6%)	$PbCl^{+}$ (17.7%)	$PbCl^{+}$ (17.6%)	$PbCl^{+}$ (17.7%)	$PbCl^{+}$ (17.8%)	$PbCl^{+}$ (17.8%)	$PbCl^{+}$ (17.9%)
Saturation Index					$\underline{Pb(OH)_2}$				
	-2.28	-3.26	-4.17	-5.13	-5.58	-6.34	-6.34	-6.44	-6.69
					$\underline{PbCO_3}$				
	-2.37	-3.35	-4.26	-5.22	-5.67	-6.43	-6.43	-6.53	-6.78

Table 2. Constants, determination coefficients (R^2) and absolute sum-of-squares (ASS) values for the pseudo-second-order model fitted to the Pb desorption data from the nonaged Pb-loaded montmorillonite in the absence or the presence of the ligands at two concentrations of 0.25 and 1 mM.[a]

Ligand concentration (mM)	Model parameter	Chelating ligand			
		No ligand	GLDA	MGDA	EDTA
0.25	q_e (mmol kg^{-1})	12.93	15.46	25.50	34.19
	k_2 (kg $mmol^{-1}$ h^{-1})	0.19	0.14	0.01	0.067
	h (mmol kg^{-1} h^{-1})	31.76	33.46	69.67	78.32
	DR_1 (mmol kg^{-1} h^{-1})	9.22	10.64	18.64	23.88
	R^2	0.98	0.91	0.91	0.97
	ASS	0.50	1.56	2.62	1.84
1.00	q_e (mmol kg^{-1})	12.93	66.17	82.69	128.5
	k_2 (kg $mmol^{-1}$ h^{-1})	0.19	0.19	0.03	0.04
	h (mmol kg^{-1} h^{-1})	31.76	83.19	205.1	660.5
	DR_1 (mmol kg^{-1} h^{-1})	9.22	36.89	60.22	107.7
	R^2	0.98	0.96	0.97	0.95
	ASS	0.50	4.05	4.38	9.38

[a]All R^2 values are significant at $P<0.001$; q_e: the quantity of Pb desorbed at equilibrium; k_2: the pseudo-second-order rate constant; *h*: the initial desorption rate, DR_1: the Pb desorption rate at t=1 hour.

Table 3. Constants, determination coefficients (R^2) and absolute sum-of-squares (ASS) values for the pseudo-second-order model fitted to the Pb desorption data from the 30-day aged Pb-loaded montmorillonite in the absence or the presence of the ligands at two concentrations of 0.25 and 1 mM.[a]

Ligand concentration (mM)	Model parameter	Chelating ligand			
		No ligand	GLDA	MGDA	EDTA
0.25	q_e (mmol kg^{-1})	2.66	3.08	3.69	9.75
	k_2 (kg $mmol^{-1}$ h^{-1})	0.8	1.05	0.92	0.32
	h (mmol kg^{-1} h^{-1})	5.66	9.96	12.52	30.42
	DR_1 (mmol kg^{-1} h^{-1})	1.82	2.36	2.85	7.39
	R^2	0.97	0.96	0.94	0.94
	ASS	0.17	0.20	0.29	0.78
1.00	q_e (mmol kg^{-1})	2.66	13.67	25.08	69.74
	k_2 (kg $mmol^{-1}$ h^{-1})	0.8	0.099	0.018	0.074
	h (mmol kg^{-1} h^{-1})	5.66	18.41	114.1	499.2
	DR_1 (mmol kg^{-1} h^{-1})	1.82	7.88	20.68	58.43
	R^2	0.97	0.97	0.99	0.98
	ASS	0.17	0.60	0.73	2.59

[a] All R^2 values are significant at $P<0.001$; q_e: the quantity of Pb desorbed at equilibrium; k_2: the pseudo-second-order rate constant; h: the initial desorption rate, DR_1: the Pb desorption rate at t=1 hour.